Characterization of Ce-doped Li_2O–ZnO–P_2O_5 Glasses for Thermal Neutron Detection

Noriaki Kawaguchi,[1*] Daisuke Nakauchi,[1] Takumi Kato,[1]
Yoshisuke Futami,[2] and Takayuki Yanagida[1]

[1]Nara Institute of Science and Technology, 8916-5 Takayama-cho, Ikoma, Nara 630-0192, Japan
[2]Department of Biological and Chemical Systems Engineering, National Institute of Technology,
Kumamoto College, 2627 Hirayamashin-Machi, Yatsushiro, Kumamoto 866-8501, Japan

We have investigated the scintillation properties of Ce-doped Li_2O–ZnO–P_2O_5 glasses. The samples were prepared using a conventional melt-quenching method with low heating temperatures from 900 to 950 °C. All the samples showed halo patterns in their X-ray diffraction (XRD) patterns. In the X-ray-induced scintillation spectra, each sample showed a single emission peak that can be ascribed to luminescence due to the 5d–4f transitions of Ce^{3+} ions. In the pulse height spectra of the samples, thermal neutron detection peaks were observed. Their light yields were estimated to be approximately 90–180 photons/neutron. Although the Ce-doped Li_2O–ZnO–P_2O_5 glasses show low light yields, they can be regarded as thermal neutron scintillators that can be produced with low heating temperatures.

1. Introduction

Ionizing radiation detection and dosimetry are commonly used in industrial, medical, and scientific fields. Radiation detectors can perform in situ radiation measurements, whereas dosimeters can measure radiation doses after radiation exposure. Different types of phosphors called scintillators and dosimetric materials are used for radiation detectors and dosimeters, respectively. Scintillation detectors are one of the most widely used radiation detectors, which consist of a photodetector and a scintillator.[1–6] Scintillators can show luminescence under ionizing radiation excitation and they are applied for medical imaging,[7] nondestructive inspection,[8,9] and well logging.[10,11] Scintillators are required to have a high light yield, a fast decay time, and a high detection efficiency. Dosimetric materials[12–15] are mainly used for personal dose monitoring.[16] These materials are required to have a human-tissue equivalency and a wide dynamic range. Studies on materials for scintillators and dosimetric materials have been intensively performed over the past decades.[2–6,12–15] This area of research is still attractive and recent studies have reported on various types of materials such as single crystals,[17–29] glasses,[30–37] sintered ceramics,[38–45] eutectic composites,[46–48] organic materials,[49,50] and organic–inorganic hybrid materials.[51,52] Among these materials, glasses are interesting research

targets due to the advantages of high formability, transparency, and degree of freedom of composition.

Glasses have been widely used as X-ray dosimetric materials, and Ag-doped phosphate glasses are commercially available.[53–55] On the other hand, glass scintillators are not widely used for X-ray and γ-ray detection; however, they are used for neutron detection, and Ce-doped lithium silicate glass[4] is commercially available. Since neutron scintillators utilize the nuclear reactions of ^{6}Li(n,α)^{3}H or ^{10}B(n,α)^{7}Li, they must contain ^{6}Li or ^{10}B. ^{6}Li, which produces higher energy, is more often used. Only a few single-crystal compositions contain Li, whereas a variety of glass compositions contain Li. However, there have been few studies on glass neutron scintillators. Intensive studies were conducted around the 1960s, and it has been reported that silicate[56] and borate[57] glasses have excellent properties. In recent years, the scintillation properties of oxyhalide glasses have been well studied, and a fluoride-phosphate (oxyfluoride) glass for neutron detection has been reported.[58] Although a phosphate glass is commercially available as a dosimeter material, there has been little investigation of the use of phosphate glasses as neutron scintillators, and their light yields under thermal neutron irradiation are unclear. In this study, we have investigated the performance of phosphate glasses as neutron scintillators. We focused on glasses with a composition of Li_2O–ZnO–P_2O_5, which contain Li_2O as a neutron converter and ZnO to suppress hygroscopicity.

2. Materials and Methods

We prepared $xCeO_2$–$10Li_2O$–$(30{-}x)ZnO$–$60P_2O_5$ (x = 1, 3, 5) glasses (hereinafter referred to as 1, 3, and 5% Ce-doped Li_2O–ZnO–P_2O_5 glasses, respectively) using the conventional melt-quenching method. As the starting materials, CeO_2, Li_2CO_3, ZnO, and $(NH_4)H_2PO_4$ powders were used. These powders were mixed and loaded into an alumina crucible. The mixed powders were melted in a crucible using an electric furnace (KDF 007EX; KDF, Kyoto, Japan) under ambient atmosphere. The heating temperature and time were changed on the basis of our visual observation of the melts. The temperature at which the melt appeared to have sufficiently low viscosity was adopted as the heating temperature for each glass. During the heating process, we observed volatile matter from the melts, which was considered to be water vapor from $(NH_4)H_2PO_4$. When we could not observe the volatile matter, we finished heating the melts. The heating temperature and time of the 1% Ce-doped Li_2O–ZnO–P_2O_5 glass were 900 °C and 20 min, whereas those of the 3 and 5% Ce-doped Li_2O–ZnO–P_2O_5 glasses were 950 °C and 10 min, respectively. It was considered that an increase in CeO_2 concentration increases the melting temperature of the Ce-doped Li_2O–ZnO–P_2O_5 glass. The melts were quenched on a stainless steel plate heated at 200 °C. As a reference sample, a commercial Ce-doped lithium silicate glass (GS20; Scintacor, Cambridge, United Kingdom) was used.

To confirm the successful preparation of the glasses, the crystalline phases of the obtained samples were investigated by X-ray diffraction (XRD) analysis. The XRD patterns of the samples were recorded using an X-ray diffractometer with a Cu-Kα X-ray source (MiniFlex600; Rigaku, Akishima, Japan). To investigate the optical properties, diffuse transmittance spectra of the samples were measured using a spectrophotometer (SolidSpec-3700; Shimadzu, Kyoto,

Japan). X-ray induced scintillation spectra of the samples were measured using our customized setup equipped with an X-ray generator, an optical fiber, and a spectrometer. X-ray irradiation of the samples was performed using an X-ray generator (XRB80P&N200X4550; Spellman High Voltage Electronics, Hauppauge, New York, United States). Luminescence from the samples was guided into a monochromator (Shamrock 163; Andor Technology, Belfast, Northern Ireland) and a CCD-based spectrometer (DU920-BU2NC; Andor Technology). We operated the X-ray generator with a tube voltage of 80 kV and a tube current of 1.2 mA. The details of this setup were presented previously.[59] Furthermore, photoluminescence (PL) excitation and emission maps, absorption spectra, and quantum yields were obtained using a PL spectrometer (Quantaurus-QY; Hamamatsu Photonics, Hamamatsu, Japan). To investigate the scintillation properties, pulse height spectra were measured. The samples were optically coupled with a photomultiplier tube (PMT; R7600U-200; Hamamatsu Photonics) using silicone grease. ^{241}Am, ^{137}Cs, and ^{252}Cf sealed sources were used for α-ray, γ-ray, and thermal neutron irradiation, respectively. The ^{252}Cf sealed source was used together with a polyethylene modulator to thermalize neutrons, with a lead brick of 50 mm thickness used to absorb γ-rays. The output signals from the PMT were amplified, shaped, and analyzed by a preamplifier (Model 113; ORTEC, Oak Ridge, United States), a shaping amplifier (Model 572; ORTEC), and a multichannel analyzer, respectively (MCA8000A; Amptek, Bedford, United Kingdom).

3. Results and Discussion

Figure 1 shows the appearance of the obtained samples. Although all the samples were transparent, small bubbles were observed in the sample bodies, which were considered to be related to the volatile matter from the melts; volatile matter remaining in a melt can form bubbles in a glass. Figure 2 shows the XRD patterns of the samples. The samples showed halo patterns and no diffraction peaks. It was considered that all the samples had a glass phase.

Figure 3 shows the diffuse transmittance spectra of the samples. We confirmed that the samples can transmit ultraviolet (UV) and visible light in the wavelength range from around 300 to 800 nm. It was considered that the absorption at around 300 nm was caused by Ce^{3+} ions because the samples with higher Ce concentrations showed absorption up to slightly longer wavelengths. Figure 4 shows the X-ray induced scintillation spectra of the samples. The samples
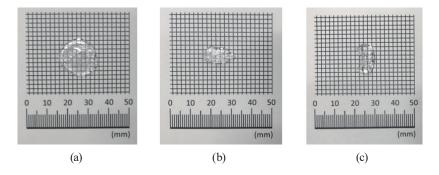

Fig. 1.   (Color online) Photographs of the (a) 1, (b) 3, and (c) 5% Ce-doped Li_2O–ZnO–P_2O_5 glasses.
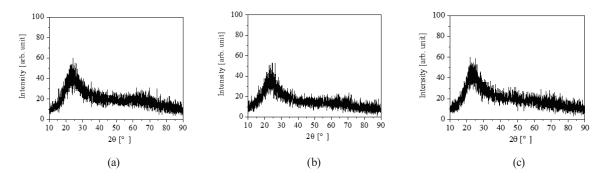
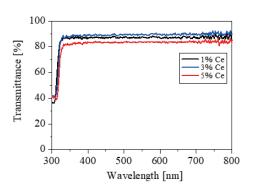Fig. 2.　(Color online) XRD patterns of the (a) 1, (b) 3, and (c) 5% Ce-doped $Li_2O–ZnO–P_2O_5$ glasses.

Fig. 3.　(Color online) Diffuse transmittance spectra of the Ce-doped $Li_2O–ZnO–P_2O_5$ glasses.

Fig. 4.　(Color online) X-ray induced scintillation spectra of the Ce-doped $Li_2O–ZnO–P_2O_5$ glasses.

show similar spectral shapes, peaking at approximately 335 nm. According to the diffuse transmittance spectra, these emissions are mostly transmitted through the sample bodies. Figure 5 shows PL excitation and emission maps of the 5% Ce-doped $Li_2O–ZnO–P_2O_5$ glass sample and GS20. Both our sample and GS20 show relatively similar emission and excitation wavelengths. The origins of the scintillation and PL peaks of the samples can be explained by the 5d–4f transitions of Ce^{3+} ions. The emission wavelengths of the samples are typical for emissions due to the 5d–4f transitions of Ce^{3+} ions in phosphate glasses. For example, the PL emission wavelengths of Ce-doped $Zn_3(PO_4)_2–Al(PO_3)_3$[60] and Ce-doped $Li_3PO_4–Al(PO_3)_3$[61] glasses are around 330 and 340 nm, respectively.

Figure 6 shows PL quantum yields and absorption spectra of the samples and GS20. The maximum PL quantum yields of the 1, 3, and 5% Ce-doped $Li_2O–ZnO–P_2O_5$ glass samples were 77.0, 79.7, and 78.1% at the excitation wavelengths of 310, 320, and 320 nm, respectively. The maximum PL quantum yields of the samples were as high as that of GS20 (80.1% at 340 nm). These yields are higher than those of other reported Ce-doped phosphate glasses prepared under ambient atmosphere. For example, Ce-doped $Zn_3(PO_4)_2–Al(PO_3)_3$[60] and Ce-doped $Li_3PO_4–Al(PO_3)_3$[61] glasses show PL quantum yields of around 30–40%. The relatively high PL quantum yields of our samples can be explained by the valence change of Ce elements. The Ce^{3+} ions can be changed to Ce^{4+} ions by heating under ambient atmosphere, which may have been the origin of the relatively low PL quantum yields reported previously. In this study, we
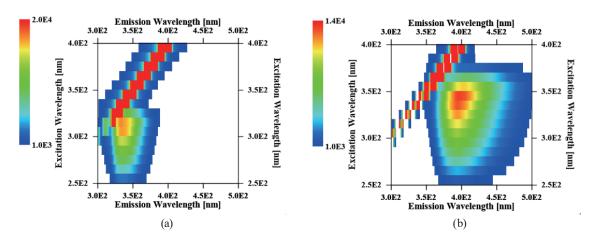
Fig. 5. (Color online) PL excitation and emission maps of the (a) 5% Ce-doped $Li_2O-ZnO-P_2O_5$ glass and (b) GS20.
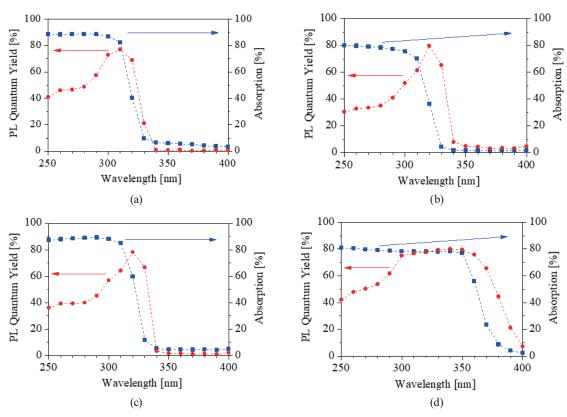

Fig. 6. (Color online) PL quantum yields and absorption spectra of the (a) 1, (b) 3, and (c) 5% Ce-doped $Li_2O-ZnO-P_2O_5$ glasses and (d) GS20.

considered that NH_3 gas generated from $(NH_4)H_2PO_4$ acted as a reducing agent ($4NH_3 + 3O_2 \rightarrow 2N_2 + 6H_2O$). Furthermore, the samples in this study were prepared with relatively low heating temperatures and short heating times (10–20 min at 900–950 °C) compared with those of Ce-doped $Zn_3(PO_4)_2-Al(PO_3)_3$ and Ce-doped $Li_3PO_4-Al(PO_3)_3$ glasses (30 min at 1300 °C). Therefore, we consider that the oxidation of Ce^{3+} to Ce^{4+} was suppressed in this study.

Figure 7 shows pulse height spectra of the 1, 3, and 5% Ce-doped Li_2O–ZnO–P_2O_5 glasses and GS20 under α-ray irradiation. All the samples and GS20 showed clear full absorption peaks. The peaks of the 1, 3, and 5% Ce-doped Li_2O–ZnO–P_2O_5 glasses and GS20 were at approximately 35, 55, 75, and 2550 channels, respectively. The light yields of the samples under α-ray irradiation were significantly lower than that of GS20.

Figure 8 shows the pulse height spectra of the 1, 3, and 5% Ce-doped samples under thermal neutron irradiation. In addition, Fig. 9 shows the pulse height spectra of the 5% Ce-doped sample and GS20 under thermal neutron and γ-ray irradiation. The 1 and 3% Ce-doped samples showed shoulder peaks and the 5% Ce-doped samples showed a peak induced by thermal neutron irradiation. Although these peaks of the samples were not very clear, the 5% Ce-doped sample showed a relatively clear detection peak at approximately 100 channels. Similarly, the 1 and 3% Ce-doped samples showed shoulder peaks at approximately 50 and 70 channels, respectively. The GS20 showed a clear peak at approximately 3400 channels under thermal neutron irradiation [Fig. 9(b)]. Defining the peak channel ratio of GS20 as 100, the peak channel ratios of the 1, 3, and 5% Ce-doped samples were 1.47, 2.06, and 2.94 under thermal neutron irradiation, respectively. Similarly, the peak channel ratios of the 1, 3, and 5% Ce-doped samples were 1.37, 2.16, and 2.94 under α-ray irradiation, respectively. The peak values under thermal neutron irradiation are considered to be consistent with those under α-ray irradiation. Since the light yield of GS20 is reported to be 6000 photons/neutron[4] and the quantum efficiencies of the PMT
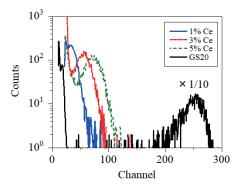

Fig. 7. (Color online) Pulse height spectra of the 1, 3, and 5% Ce-doped Li_2O–ZnO–P_2O_5 glasses and GS20 under α-ray irradiation from [241]Am.
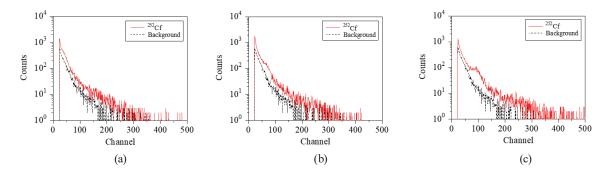

(a)

(b)

(c)

Fig. 8. (Color online) Pulse height spectra of the (a) 1, (b) 3, and (c) 5% Ce-doped Li_2O–ZnO–P_2O_5 glasses under thermal neutron irradiation from [252]Cf.
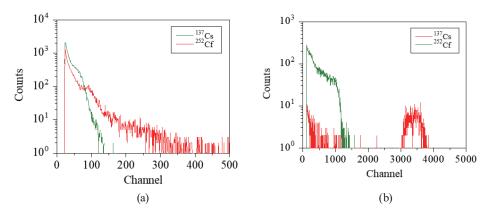
Fig. 9.   (Color online) Pulse height spectra of the (a) 5% Ce-doped $Li_2O-ZnO-P_2O_5$ glass and (b) GS20 under γ-ray and thermal neutron irradiation from ^{137}Cs and ^{252}Cf.

in this study are not markedly different between the samples and GS20 at the emission wavelengths, the light yields of the 1, 3, and 5% Ce-doped samples were estimated to be approximately 90, 120, and 180 photons/neutron, respectively. In Fig. 9, no photoelectric absorption peaks were clearly observed under γ-ray irradiation from ^{137}Cs. The Compton edges of the 5% Ce-doped sample and GS20 under γ-ray irradiation from ^{137}Cs were observed at 70 and 1100 channels, respectively. We calculated the values obtained by dividing each peak channel number under thermal neutron irradiation by the corresponding channel number of the Compton edge. The obtained values of the 5% Ce-doped sample and GS20 were 1.43 and 3.09, respectively. Since the n/γ ratio of GS20 is reported to be approximately 0.3,[4] the n/γ ratio of the 5% Ce-doped sample was estimated to be approximately 0.14.

Although the Ce-doped $Li_2O–ZnO–P_2O_5$ glass samples show high PL quantum yields, they show significantly lower light yields than GS20. This can be explained using the following equation:[3]

$$N_{ph} = (E_{ab}/\beta \cdot E_g) \cdot S \cdot Q,   \tag{1}$$

where N_{ph} is the number of scintillation photons, E_{ab} is the absorbed energy, $\beta \cdot E_g$ is the energy required to generate a single electron–hole pair (β is a constant and E_g is the band gap energy), S is the transport efficiency of electron–hole pairs, and Q is the quantum efficiency of the luminescence centers. For the Ce-doped $Li_2O–ZnO–P_2O_5$ glass samples, Q is considered to be high but S is considered to be low. There is a possibility that the Ce-doped $Li_2O–ZnO–P_2O_5$ glass samples contain large numbers of trapping centers. Despite the low light yields, Ce-doped $Li_2O–ZnO–P_2O_5$ glasses can be regarded as attractive glass neutron scintillators because they can be prepared with low heating temperatures. Further developments are expected.

4.   Conclusions

The scintillation properties of Ce-doped $Li_2O–ZnO–P_2O_5$ glasses were studied. We prepared 1, 3, and 5% Ce-doped $Li_2O–ZnO–P_2O_5$ glasses with low heating temperatures (900–950 °C)

using the conventional melt-quenching method. The Ce-doped Li_2O–ZnO–P_2O_5 glasses showed halo patterns and no diffraction peaks in their XRD patterns. From their diffuse transmittance spectra and X-ray induced scintillation spectra, we confirmed that these glass bodies can transmit their emissions. On the basis of the PL excitation and emission maps, we explained the luminescence as being due to 5d–4f transitions of Ce^{3+} ions. The PL and scintillation properties were evaluated by comparison with those of a commercial Ce-doped lithium silicate glass (GS20). The maximum PL quantum yields of the 1, 3, and 5% Ce-doped Li_2O–ZnO–P_2O_5 glasses and GS20 were 77.0, 79.7, 78.1, and 80.1%, respectively. The light yields of the 1, 3, and 5% Ce-doped Li_2O–ZnO–P_2O_5 glasses were estimated to be approximately 90, 120, and 180 photons/neutron, respectively, which were lower than that of GS20 (6000 photons/neutron). The n/γ ratio of the 5% Ce-doped Li_2O–ZnO–P_2O_5 glass was estimated to be approximately 0.14. Although the light yields of the Ce-doped Li_2O–ZnO–P_2O_5 glasses were low, the glasses can act as thermal neutron scintillators.

Acknowledgments

References

1   G. F. Knoll: Radiation Detection and Measurement (Wiley, New York, 2010) 4th ed.
2   S. E. Derenzo, M. J. Weber, E. Bourret-Courchesne, and M. K. Klintenberg: Nucl. Instrum. Methods Phys. Res., Sect. A **505** (2003) 111.
3   C. W. E. van Eijk: Nucl. Instrum. Methods Phys. Res., Sect. A **460** (2001) 1.
4   C. W. E. van Eijk, A. Bessière, and P. Dorenbos: Nucl. Instrum. Methods Phys. Res., Sect. A **529** (2004) 260.
5   C. W. E. van Eijk: IEEE T. Nucl. Sci. **59** (2012) 2242.
6   T. Yanagida: Opt. Mater. **35** (2013) 1987.
7   C. W. E. van Eijk: Phys. Med. Biol. **47** (2002) R85.
8   R. S. Holt, M. J. Cooper, and D. F. Jackson: Nucl. Instrum. Methods **221** (1984) 98.
9   K. Watanabe, K. Matsumoto, A. Uritani, K. Hitomi, M. Nogami, and W. Kockelmann: Sens. Mater. **32** (2020) 1435.
10   C. L. Melcher: Nucl. Instrum. Methods Phys. Res., Sect. B **40/41** (1989) 1214.
11   N. Kawaguchi, G. Okada, K. Fukuda, and T. Yanagida: Nucl. Instrum. Methods Phys. Res. Sect. A **954** (2018) 161518.
12   S. W. S. McKeever: Thermoluminescence of Solids (Cambridge University Press, Cambridge, 1985).
13   E. G. Yukihara and S. W. S. McKeever: Optically Stimulated Luminescence (Wiley, Chichester, UK, 2011).
14   S. W. S. McKeever: Nucl. Instrum. Methods Phys., Res. Sect. B **184** (2001) 29.
15   T. Yanagida, G. Okada, and N. Kawaguchi: J. Lumin. **207** (2019) 14.
16   P. Covens, D. Berus, N. Buls, P. Clerinx, and F. Vanhavere: Radiat. Prot. Dosimetry **124** (2007) 250.
17   N. Kawaguchi, H. Kimura, M. Akatsuka, G. Okada, N. Kawano, K. Fukuda, and T. Yanagida: Sens. Mater. **30** (2018) 1585.
18   N. Kawaguchi, N. Kawano, G. Okada, and T. Yanagida: J. Lumin. **206** (2019) 634.
19   T. Yanagida, Y. Fujimoto, M. Arai, M. Koshimizu, T. Kato, D. Nakauchi, and N. Kawaguchi: Sens. Mater. **32** (2020) 1351.
20   P. Kantuptim, M. Akatsuka, M. Koshimizu, D. Nakauchi, T. Kato, N. Kawaguchi, and T. Yanagida: Sens. Mater. **32** (2020) 1357.

21   M. Akatsuka, D. Nakauchi, T. Kato, N. Kawaguchi, and T. Yanagida: Sens. Mater. **32** (2020) 1373.

22   D. Nakauchi, T. Kato, N. Kawaguchi, and T. Yanagida: Sens. Mater. **32** (2020) 1389.

23   Y. Takebuchi, H. Fukushima, D. Nakauchi, T. Kato, N. Kawaguchi, and T. Yanagida: Sens. Mater. **32** (2020) 1405.

24   N. Kawaguchi, G. Okada, Y. Futami, D. Nakauchi, T. Kato, and T. Yanagida: Sens. Mater. **32** (2020) 1419.

25   Y. Fujimoto, D. Nakauchi, T. Yanagida, M. Koshimizu, and K. Asai: Sens. Mater. **33** (2021) 2147.

26   P. Kantuptim, H. Fukushima, H. Kimura, D. Nakauchi, T. Kato, M. Koshimizu, N. Kawaguchi, and T. Yanagida: Sens. Mater. **33** (2021) 2195.

27   D. Nakauchi, T. Kato, N. Kawaguchi, and T. Yanagida: Sens. Mater. **33** (2021) 2203.

28   H. Fukushima, M. Akatsuka, H. Kimura, D. Onoda, D. Shiratori, D. Nakauchi, T. Kato, N. Kawaguchi, and T. Yanagida: Sens. Mater. **33** (2021) 2235.

29   M. Akatsuka, H. Kimura, D. Onoda, D. Shiratori, D. Nakauchi, T. Kato, N. Kawaguchi, and T. Yanagida: Sens. Mater. **33** (2021) 2243.

30   N. Kawaguchi, D. Nakauchi, S. Hirano, N. Kawano, G. Okada, K. Fukuda, and T. Yanagida: Jpn. J. Appl. Phys. **57** (2018) 02CB13.

31   N. Kawaguchi and T. Yanagida: Sens. Mater. **31** (2019) 1257.

32   N. Kawaguchi and T. Yanagida: Jpn. J. Appl. Phys. **59** (2020) SCCB21.

33   D. Shiratori, D. Nakauchi, T. Kato, N. Kawaguchi, and T. Yanagida: Sens. Mater. **32** (2020) 1365.

34   H. Masai, T. Ina, H. Kimura, N. Kawaguchi, and T. Yanagida: Sens. Mater. **33** (2021) 2155.

35   T. Kato, D. Shiratori, M. Iwao, H. Takase, D. Nakauchi, N. Kawaguchi, and T. Yanagida: Sens. Mater. **33** (2021) 2163.

36   T. Yanagida, Y. Fujimoto, H. Masai, G. Okada, T. Kato, D. Nakauchi, and N. Kawaguchi: Sens. Mater. **33** (2021) 2179.

37   N. Kawaguchi, H. Masai, M. Akatsuka, D. Nakauchi, T. Kato, and T. Yanagida: Sens. Mater. **33** (2021) 2215.

38   H. Kimura, D. Nakauchi, T. Kato, N. Kawaguchi, and T. Yanagida: Sens. Mater. **32** (2020) 1381.

39   T. Kato, D. Nakauchi, N. Kawaguchi, and T. Yanagida: Sens. Mater. **32** (2020) 1411.

40   D. Maruyama, S. Yanagisawa, Y. Koba, T. Andou, and K. Shinsho: Sens. Mater. **32** (2020) 1461.

41   S. Yanagisawa, D. Maruyama, R. Oh, Y. Koba, T. Andoh, and K. Shinsho: Sens. Mater. **32** (2020) 1479.

42   A. Ishikawa, A. Yamazaki, K. Watanabe, S. Yoshihashi, A. Uritani, Y. Sakurai, H. Tanaka, R. Ogawara, M. Suda, and T. Hamano: Sens. Mater. **32** (2020) 1489.

43   R. Oh, S. Yanagisawa, H. Tanaka, T. Takata, G. Wakabayashi, M. Tanaka, N. Sugioka, Y. Koba, and K. Shinsho: Sens. Mater. **33** (2021) 2129.

44   D. Shiratori, T. Kato, D. Nakauchi, N. Kawaguchi, and T. Yanagida: Sens. Mater. **33** (2021) 2171.

45   H. Kimura, T. Kato, D. Nakauchi, N. Kawaguchi, and T. Yanagida: Sens. Mater. **33** (2021) 2187.

46   N. Kawaguchi, K. Fukuda, T. Yanagida, Y. Fujimoto, Y. Yokota, T. Suyama, K. Watanabe, A. Yamazaki, and A. Yoshikawa: Nucl. Instrum. Methods Phys. Res., Sect. A **652** (2011) 209.

47   N. Kawaguchi, H. Kimura, Y. Takebuchi, D. Nakauchi, T. Kato, and T. Yanagida: Radiat. Meas. **132** (2020) 106254.

48   N. Kawaguchi, H. Kimura, D. Nakauchi, T. Kato, and T. Yanagida: J. Ceram. Soc. Jpn. **129** (2021) 402.

49   M. Koshimizu, T. Yanagida, R. Kamishima, Y. Fujimoto, and K. Asai: Sens. Mater. **31** (2019) 1233.

50   A. Watanabe, A. Magi, M. Koshimizu, A. Sato, Y. Fujimoto, and K. Asai: Sens. Mater. **33** (2021) 2251.

51   A. Horimoto, N. Kawano, D. Nakauchi, H. Kimura, M. Akatsuka, and T. Yanagida: Sens. Mater. **32** (2020) 1395.

52   M. Koshimizu, N. Kawano, A. Kimura, S. Kurashima, M. Taguchi, Y. Fujimoto, and K. Asai: Sens. Mater. **33** (2021) 2137.

53   Y. Miyamoto, T. Yamamoto, K. Kinoshita, S. Koyama, Y. Takei, H. Nanto, Y. Shimotsuma, M. Sakakura, K. Miura, and K. Hirao: Radiat. Meas. **45** (2010) 546.

54   H. Nanto, Y. Miyamoto, T. Oono, Y. Takei, T. Kurobori, and T. Yamamoto: Procedia Eng. **25** (2011) 231.

55   Y. Miyamoto, H. Nanto, T. Kurobori, Y. Fujimoto, T. Yanagida, J. Ueda, S. Tanabe, and T. Yamamoto: Radiat. Meas. **71** (2014) 529.

56   A. R. Spowart: Nucl. Instrum. Methods **75** (1969) 35.

57   A. M. Bishay: J. Am. Ceram. Soc. **44** (1961) 231.

58   A. Fukabori, T. Yanagida, V. Chani, F. Moretti, J. Pejchal, Y. Yokota, N. Kawaguchi, K. Kamada, K. Watanabe, T. Murata, Y. Arikawa, K. Yamanoi, T. Shimizu, N. Sarukura, M. Nakai, T. Norimatsu, H. Azechi, S. Fujino, H. Yoshida, and A. Yoshikawa: J. Non-Cryst. Solids **357** (2011) 910.

59   T. Yanagida, K. Kamada, Y. Fujimoto, H. Yagi, and T. Yanagitani: Opt. Mater. **35** (2013) 2480.

60   S. Hirano, T. Kuro, H. Tatsumi, G. Okada, N. Kawaguchi, and T. Yanagida: J. Mater. Sci. Mater. Electron. **28** (2017) 6064.

61   H. Tatsumi, G. Okada, T. Yanagida, and H. Masai: J. Ceram. Soc. Jpn. **124** (2016) 550.